Phase constitution of kaolin-based refractory concrete castables containing spinel or mullite (preformed and insitu) additives

Morsy M. Abou-Sekkina[1,*], Salah A. Abo-El-Enein[2], Nagy M. Khalil[3] and Osama A.Shalma[4]

[1]Department of Chemistry, Faculty of Science, Tanta University, Tanta, Egypt.
[2]Department of Chemistry, Faculty of Science, Ain Shams University, Cairo, Egypt.
[3]Refractories, Ceramics and Building Materials Department, National Research Center (NRC), Giza, Egypt.
[4]Environmental Monitoring Laboratory, Tanta, Egypt.

ABSTRACT

The present maniscrupt aimed to improve the castable refractory castable concretes. Thus, kaolin-based refractory castables investigated were carefully prepared. They are composed of 90 wt. % well-graded (coarse, medium, and fine) kaolin aggregate, 10 wt. % binding matrix and adequate amount of distilled water. The binder mixture was calcium aluminate cement (CAC) containing 80 % Alumina and magnesium-aluminate spinel (MA- spinel) or mullite either preformed or insitu. The castable batches were cast into cubes (25 x 25 x 25 mm), cured for 7 days under water, and followed by drying at 110ºC for 24 hrs. The samples were then subjected to firing at 1550°C for a soaking time of 1 hr. The phase composition of the prepared castable samples were investigated by using X-Ray diffraction (XRD) analysis, scanning electron microscopy (SEM), energy dispersive X-ray (EDX) analysis, differential thermal analysis (DTA) and thermal gravimetric analysis (TGA). Results of these investigations confirm each other.

Introduction

A range of lime-free castables, predominantly based on MgO-SiO$_2$, Al$_2$O$_3$-SiO$_2$ and MgO-Al$_2$O$_3$ bond systems, has been developed and resulted in suitable high-temperature properties via the formation of refractory compounds such as mullite (3Al$_2$O$_3$.2SiO$_2$) and MA-spinel (MgO.Al$_2$O$_3$) [1]. The conventional method of the preparation of MA spinel is solid state sintering between high purity MgO and Al$_2$O$_3$ where the temperature needed is normally between 1200 and 1400°C for commercial practice [2 and 3]. The self-forming (insitu) spinel is fabricated during service by reaction of fine magnesia (MgO) additions with alumina present in the matrix fines, often in the calcium aluminate cement. Very often small amount of microsilica is added to the insitu spinel bonded castable to promote hydration resistance [2, 4 and 5]. Mullite (3Al$_2$O$_3$-2SiO$_2$) is a characteristic, strong and thermo-dynamically stable product in the high temperature solid-state reaction between silica (SiO$_2$) and alumina (Al$_2$O$_3$) [6-9]. In low and ultra low cement concretes (LCC and ULCC), fine silica and alumina powders, contained in their matrices, lead on firing to form insitu mullite in the bond phase as a network of needles at $\geq$ 1300°C. The elongated needle-like mullite crystals grow and lock the structure to create a strong refractory bond system so improving the mechanical properties of the castable and strengths the microstructure of the binding matrix [10-12].

The properties of refractory concretes or castables are largely dependent upon the choice of refractory aggregate and hydraulic cement used. In principle, all refractory grains can be used in refractory concrete as aggregates but in practice most aggregates contain mainly alumina and silica in various forms [13].

Experimental procedures

The starting materials used in this investigation are: calcium aluminate cement (Alcoa, CA-25R- 80 % Alumina), Egyptian kaolin aggregate, preformed MA-spinel (MgO.Al$_2$O$_3$), preformed mullite (3Al$_2$O$_3$-2SiO$_2$), magnesium oxide MgO (BDH), silica SiO$_2$ ($\geq$ 96 %) and calcined aluminum oxide Al$_2$O$_3$ (Alcoa).

The refractory aggregate (kaolin) were well graded as 65 wt. % coarse (2.36-0.50 mm), 10 wt. % medium (0.50-0.25 mm) and 25 wt. % fine (< 0.25 mm). The refractory castable samples were prepared according to the compositions represented in Tables 1, where a 90 wt. % well-graded aggregate intermixed with the binding matrix and adequate amounts of distilled water according to the standard "good ball in hand" ASTM C-860 method. The mixed batches were then cast into cubes of 25 mm side length in steel moulds and left in their moulds at 100 % relative humidity for 24 hrs. The samples were then demoulded and further cured for 7 days under water, followed by drying at 110ºC for 24 hrs. Finally the samples were subjected to firing at 1550°C in an electric muffle furnace for a soaking time of 1 hr.

The refractory castable samples were characterized using X-ray diffraction (XRD) analysis where PHILIPS "PW 1840" diffractometer with Cu-kα radiation and Ni-filter. PHILIPS "PW 1729" X-ray generator and PHILIPS "PW 8203A" recorder (at a scan speed 0.1°, 2θ from 5° to 100°, slit 0.2) are used. Selected castable samples were subjected to scanning electron microscopy (SEM). A "JEOL JXA-840" high resolution scanning electron microscope was used.

The 7-days cured samples were crushed (after drying), finely ground, and then subjected to DTA and TGA. This investigation was carried out using a "Shimadzu DTA-50" and

"Shimadzu TGA-50" thermal analyzers. Each sample was heated in Nitrogen atmosphere (Rate flow of N_2: 20 ml / min.) from the ambient temperature to 1000°C with heating rate of 10°C/min.

Results and discussion

Microstructure of the fired castables

The phase composition of the kaolin-based (K0, K2, K8, K5 and K11) castable specimens sintered at 1550°C for 1hr, were investigated by means of X-ray diffraction (XRD) analysis and scanning electron microscope (SEM).

The XRD patterns of the kaolin-based castable specimens K0, K2, K8, K5 and K11 are shown in the Figs. (1 and 2).
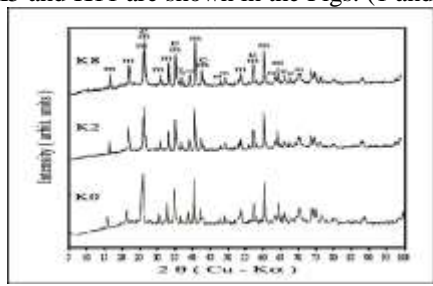
Fig (1): X-Ray Diffraction patterns of castables K0, K2 and K8 fired at 1550°C for 1hr (c : corundum, m : mullite).
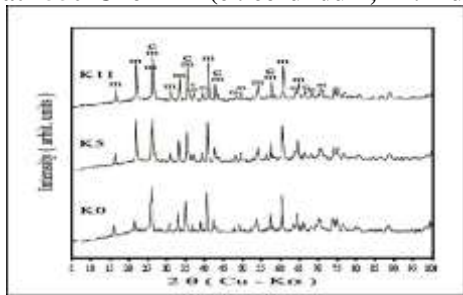
Fig (2): X-Ray Diffraction patterns of castables K0, K5 and K11 fired at 1550°C for 1hr (c : corundum, m : mullite).

The castable sample K0 was considered as the control castable sample. The XRD patterns indicated that all the castable specimens composed mainly of transformed mullite phase along with some peaks characterizing the corundum phase. Other minor phases, CAC and spinel (preformed or insitu), present in small quantities and could not be detected by XRD analysis. The SEM micrographs of the kaolin-based castable specimens K2, K8, K5 and K11 are shown in Figs. (3-6).
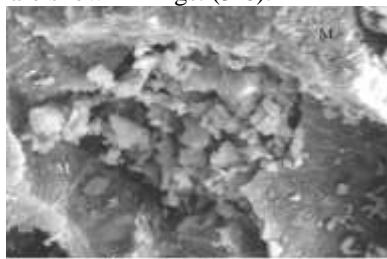
Fig (3): SEM photomicrographs of K2 castable sample fired at 1550°C for 1 hr (C: corundum grains, M: needle-shaped mullite).

They show that the kaolin particles are usually stacked together to form agglomerates, and the irregular Al_2O_3 particles are dispersed in the matrix. The primary mullite appears to grow from the kaolin raw materials with a rod-like shape [14]. Mullite and corundum phases appeared as result of sintering of castable samples at 1550°C for 1hr where kaolinite ($Al_2O_3.2SiO_2.2H_2O$), the essential component of kaolin, lost the OH units in its crystal structure at around 450°C, forming an almost amorphous

material known as metakaolinite ($Al_2O_3.2SiO_2$). Metakaolinite structure is unstable and at about 1000°C it is transformed to γ-alumina, cristoballite (SiO_2) and primary mullite crystals. At higher temperatures, the crystals of primary mullite grow by reacting with amorphous aluminosilicate phase forming secondary mullite [15 and 16]. The impurities distort the atomic structure and assist the formation of liquid phase at higher firing temperatures.

Fig (4): SEM photomicrographs of K8 castable sample fired at 1550°C for 1 hr (C: corundum grains, M: needle-shaped mullite).
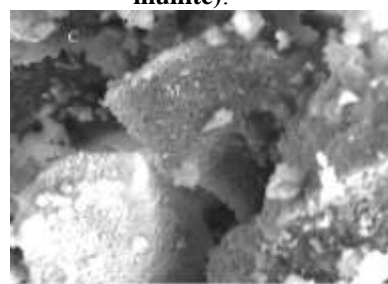
Fig (5): SEM photomicrographs of K5 castable sample fired at 1550°C for 1 hr (C: corundum grains, M: needle-shaped mullite).
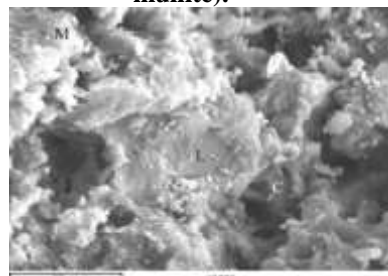
Fig. (6): SEM photomicrographs of K11 castable sample fired at 1550°C for 1 hr (C: corundum grains, M: needle-shaped mullite, L: liquid phase).

Brindley and Nakahira [17] reported that when kaolinite sample is heated up to 1050°C, the transformation from kaolinite to mullite can be explained by the following reactions:

$$Al_2O_3.2SiO_2.2H_2O \xrightarrow{400-\approx 500°C} (Al_2O_3.2SiO_2) + H_2O$$
$$\text{Kaolinite} \qquad\qquad \text{metakaolinite}$$

$$2(Al_2O_3.2SiO_2) \xrightarrow{\approx 950°C} Si_3Al_4O_{12} + SiO_2$$
$$\text{metakaolinite} \qquad (\text{Al-Si spinel})$$
$$(\text{amorphous})$$

$$3Si_3Al_4O_{12} \xrightarrow{>1050°C} 2(3Al_2O_3.2SiO_2) + 5SiO_2$$
$$(\text{Al-Si spinel}) \qquad\qquad \text{mullite}$$
$$(\text{amorphous})$$
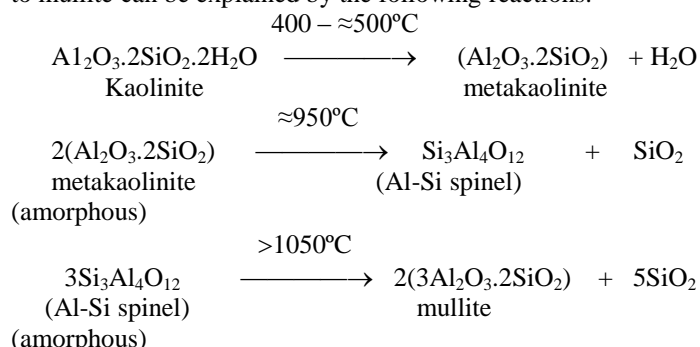
Differential Thermal Analysis (DTA) and Thermal Gravimetric Analysis (TGA):

The results of thermal analyses by thermogravimetric analysis (TGA) and differential thermal analysis (DTA) of castable sample K0 (the control castable sample), hydrated for 7

days are shown in Fig. (7).
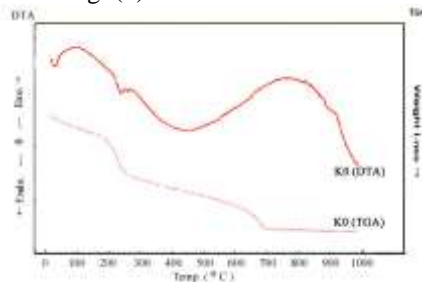
Fig. (7): Thermal analyses (TGA and DTA) of castable sample K0, hydrated for 7 days.

Castable sample K0 displays DTA endotherms at ≈ 35°C, 240°C, 261°C and broad endotherm in the region 285°C to 682°C. The TG thermogram of the castable sample K0 is from room temperature to 1000°C. The stages of weight loss are showed in Table (2). The total weight loss was 3.397 % from room temperature to 700 °C.

Kaolin-based Castable Samples Containing Spinel (Preformed or In situ):

Fig. (8; A, B and C) shows the DTA thermograms of castable samples couples (hydrated for 7 days) K1, K7; K2, K8; and K3, K9, respectively.

They show DTA endotherms at ≈35°C to 40°C, ≈245°C, ≈275°C and broad endotherms in the region ≈275°C to ≈800°C.

(A)

(B)

(C)
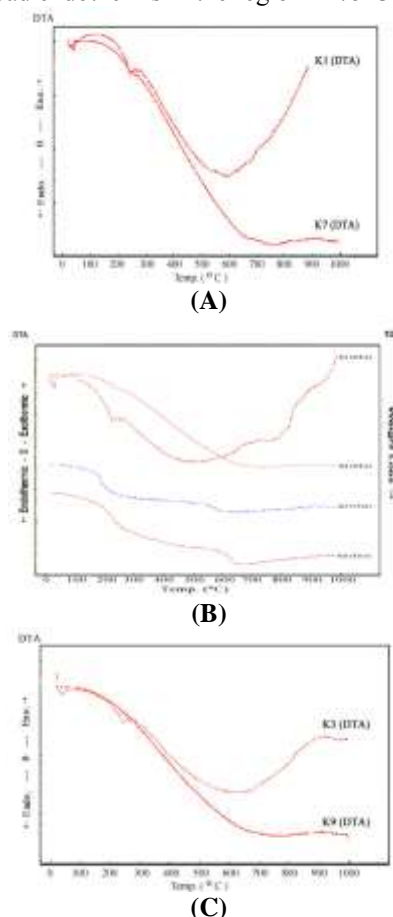
Fig. (8): Differential thermal analysis (DTA) of castable samples couples K1, K7 (A)**; K2, K8** (B)**; and K3, K9** (C)**, respectively.**

The TGA thermograms of the castable samples K2 and K8 are from room temperature to 1000 °C. The stages of percentage weight loss are shown in Table (3). The total weight loss of both castable samples was 1.721 % and 3.306 %, respectively, as measured from room temperature to 700°C.

Kaolin-based Castable Samples Containing Mullite (Preformed or In situ):

Fig. (9; A, B and C) shows the DTA thermograms of castable samples couples (hydrated for 7 days) K4, K10; K5, K11; and K6, K12, respectively.

They show DTA endotherms at ≈35°C, ≈245°C, ≈280°C and broad endotherms in the region ≈280°C to ≈900°C.

(A)

(B)

(C)
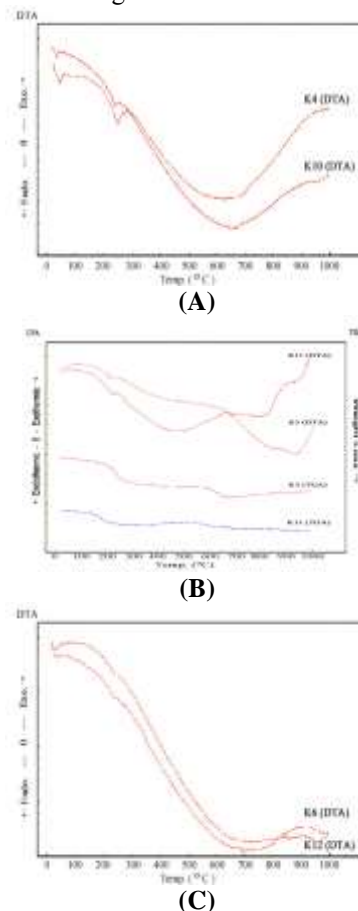
Fig. (9): Differential thermal analysis (DTA) of castable samples couples K4, K10 (A); K5, K11 (B); and K6, K12 (C), respectively.

The TGA thermograms of castable samples K5 and K11 are from room temperature to 1000°C. The stages of percentage weight loss are shown in Table (4). The total weight loss of both castable samples was 2.569 % and 0.748 %, respectively, as measured from room temperature to 700 °C.

The DTA endotherms formed in the temperature range up to ≈ 250°C are due to the release of free or the physically bound (absorbed) water [18- 20]. The endotherms at 250°C to 450°C are due to expulsion and oxidation of the volatile organic compounds. The hexagonal hydrates CAH_{10} (the main hydration product of CA and CA_2 phases) and C_2AH_8 are meta-stable under the influence of temperature conversion into the stable cubic hydrates C_3AH_6 (katoite) and AH_3 (gibbsite) [21]. The dual endotherms occurring in the temperature range 250 to 350°C represent dehydration reactions involving (AH_3) and C_3AH_6 [22 and 23].

As the temperature goes up, the kaolinite undergoes dehydroxylation and recrystallization. Dehydroxylation that occurs on the phase boundary [16] produces a broad endothermic reaction in the 500-600°C range. Dehydroxylation begins at the temperature ≈ 450°C and continues up to around 700°C [18, 24-27] or ≈ 800°C [28]; and it can be shifted to the temperature ≈ 420 °C [29]. The endotherm revealed in this

temperature range corresponds to loss of the hydroxyl units (removal of the chemically bound water) and complete expulsion of the structure water of the kaolinite structure, forming an almost amorphous material identified as metakaolin [16, 18, 30 and 31], whereas recrystallization of the resulting metakaolinite to cristoballite (SiO_2) and γ-Al_2O_3 or mullite produces an exothermic reaction between 950 and 1050°C.

The mechanism of dehydroxylation includes a transport of OH- groups to the phase boundary, then the reaction of the groups on the boundary and, finally, transport of the products (H_2O molecules) to the edge of the crystal. It was revealed, that this process is diffusion of the H_2O molecules between layers of the kaolinite structure [16]. That is to say, it occurs through diffusion-controlled mechanism. Because of the condition that 2/3 of the OH groups in the octahedral layer are on the surface of the layer and 1/3 of the OH groups are inside, two different activation energies of dehydroxylation can exist [32]. Liberation of the outer OH groups appears at the temperature 420 - 600°C, and the liberation of the inner OH groups appears at higher temperatures as far as 850 - 950°C [33-36].

A chemical equation of dehydroxylation can be represented by several ways. The chemical equations describing this process are:

$$(Al_2O_3.2SiO_2.2H_2O) \rightarrow (Al_2O_3.2SiO_2) + 2H_2O \text{ (g)},$$
$$Al_2Si_2O_5(OH)_4 \rightarrow Al_2Si_2O_7 + 2H_2O(g); \quad \text{or}$$

considering that in a unit cell there are eight OH groups, which undergo the following change:

$$8OH^- \rightarrow 4H_2O \text{ (g)} + 4O^{2-} \qquad [16]$$

Metakaolinite with its new structure in the crystals is created at the temperature range of 420 - 740°C [27].

The exotherm at 900 - 1000°C reflects the formation of crystalline product (spinel phase) from the amorphous intermediate phase.

Upon further heating, sintering reactions took place and mullite formation, γ-alumina and cristoballite (SiO_2) are observed [18, 30, 31 and 37].

The compositions prepared were designed to evaluate and detect the effect of the added spinel or mullite to improve the final castable products. This could be obviously seen and supported from results of TGA and DTA thermal analyses (as shown in Figs 8 and 9 comparing with Fig. 7) . In the sense that Figs 8 and 9 display induced gradual thermal stability as functions of the added additives (spinel or mullite) causing a displacement of TG and DTA thermograph peaks towards higher temperatures. Consequantely these, of course, may induce high refractoriness and hence high mechanical proerties durability of the castable products.

Conclusions

The main conclusions derived from these investigations are summarized as follows:

1. The X-ray diffraction patterns of the kaolin-based castable samples indicated that they composed mainly of transformed mullite phase along with some peaks characterizing the corundum phase. Other minor phases, CAC and additive (added spinel or mullite; preformed or in situ), are present in small quantities could not be detected by XRD analysis.

2. The SEM micrographs show that the kaolin particles usually stack together to form agglomerates, and the irregular Al_2O_3 particles disperse in matrix. The primary mullite appears to grow from the kaolin raw materials with a rod-like shape. The secondary mullite also grows to an elongated shape.

3. The differential thermal analyses (DTA) and thermogravimetric (TGA) measurements of kaolin-based castable samples containing spinel and mullite (preformed or insitu) are mainly the thermal analysis of kaolin (the main constituent of the castable samples, 90 wt. %).

4. In general, the DTA curve of each kaolin-based castable sample show three endotherms in the temperature range between room temperature and $\approx$ 265°C and broad endotherm in the region $\approx$280°C to $\approx$820°C.

5. The DTA endotherms formed in the temperature range up to $\approx$250 °C are due to the release of free or the physically absorbed water. The endotherms at 250°C to 450°C are due to expulsion and oxidation of the volatile organic compounds. The dual endotherms occurring in the temperature range 250-350°C represent dehydration reactions involving (AH_3) and C_3AH_6. The kaolinite undergoes dehydroxylation and recrystallization producing a broad endothermic reaction in the 500°C - 600°C range.

References

[1] F. Cunha and R. Bradt, Electric Furnace Conference Proceedings, 143-152, (1999).

[2] M. Fuhrer, A. Hey and W. Lee, *"Microstructural evolution in self-forming spinel/calcium aluminate-bonded castable refractories",* J. Europ. Ceram. Soc., 18 (15), 813-821, (1998).

[3] S. Mukhopadhyay, S. Sen, T. Maiti, M. Mukherjee, R. Nandy and B. Sinhamahapatra, *"Insitu spinel bonded refractory castable in relation to co-precipitation and sol–gel derived spinel forming agents",* Ceram. Inter., 29(8), 857-868, (2003).

[4] Y. Ko, *"Influence of the characteristics of spinels on the slag resistance of Al_2O_3-MgO and Al_2O_3-spinel castables",* J. Amer. Ceram. Soc., 83(9), 2333-2335, (2000).

[5] C. Parr, T. Beir, M. Vialle and C. Revais, *"An approach to formulate spinel forming castables",* in: Proceedings of the Unified International Technical Conference on Refractories (UNITECR' 99), Berlin, Germany, 19-21, (1999).

[6] W. Kronert, and U. Schumacher, *"Use of low-cement and ultralow-cement refractory castables in the iron and steel industry furnace prospects",* Interceram, (Aachen Proc. 1988), 3(8), 12–18, (1989).

[7] A. Hundere and B. Myhre, *"Effect of different finest fractions (SiO_2 and Al_2O_3) in alumina based ultra low cement castables",* Elkem Refractories, Presented at the Amer. Ceram. Soc. 98th annual meeting in Indianapolis, (1996).

[8] Y. Pivinski, *"New refractory concretes and binding systems",* Refract. Ind. Ceram., 39(314), 91-99, (1998).

[9] S. Moehmel, W. Gessner, A. Bier and C. Parr, *"The influence of micro silica on the course of hydration of mono-calcium aluminate",* in: Proc. Inter. Conf., Calcium Aluminate Cements, IOM Communications, London, 319-330, (2001).

[10] B. Myhre, *"Strength development of bauxite-based ultralow-cement castables",* Amer. Ceram. Soc. Bull., 73(5), 68-73, (1994).

[11] B. Sandburg and B. Myhre, *"Castables in the system MgO-Al_2O_3-SiO_2",* in: Proceedings of the Unified International Technical Conference on Refractories (UNITECR' 95), Kyoto, Japan, 173-179, (1995).

[12] M. Hundere and B. Myhre, *"Substitution of reactive alumina with microsilica in low cement and ultra low cement castables",* in: Proceedings of the Unified International Technical Conference on Refractories (UNITECR' 97), New Orleans, USA, 91-100, (1997).

[13] L. Girgis, S. El-Hemaly and N. Khalil, Inter. ceram., 52(3), 140-144, (2003).

[14] Y. Chen, M. Wang and M. Hon, *"Secondary mullite formation in kaolin–Al2O3 ceramics"*, J. Mater. Res., 19, 3, (2004).

[15] S. Agathopoulos, H. Fernandes, D. Tulyaganov, and J. Ferreira, *"Preparation of mullite whiskers from kaolinite using CuSO₄ as fluxing agent"*, Mater. Scie. Forum, 455-456, 818-821, (2004).

[16] I. Štubňa, G. Varga and A. Trník, *"Investigation of kaolinite dehydroxylations is still interesting"*, Építôanyag ,58, évf. 1, szám, (2006).

[17] G. Brindley and M. Nakahira, *"The kaolinite–mullite reaction series: I., II and III"* J. Amer. Ceram. Soc., 42, 311-324, (1959).

[18] S. Sayin, *"Origin of kaolin deposits: Evidence from the Hisarcik (Emet-Kutahya) deposits, Western Turkey"*, Turkish J. Earth Sci., 16, 77-96, (2007).

[19] F. Huertas, E. Huertas and J. Linares, *"Hydrothermal synthesis of kaolinite: Method and characterization of the synthetic materials"*, Appl. Clay Sci., 7:345-356, (1993).

[20] G. Saviano, M. Violo, U. Pieruccini and E. da Silva, *"Kaolin deposits from the northern sector of the Cunene anorthosite complex (southern Angola)"*, Clays and Clay Minerals, 53, 6, 674-685, (2005).

[21] I. Pundiene, S. Goberis, V. Antonovic, R. Stonys and A. Špokauskas, *"Carbonation of alumina cement-bonded conventional refractory castable in fireplace"*, Mater. Scie. (Medziagotyra), 12(4), (2006).

[22] V. Ramachandran, R. Feldman and P. Sereda, *"Application of Differential Thermal Analysis in Cement Research"*, Research Paper No. 249 of the Division of Building Research, National research Council Canada, and Highway Research Record no.62, 40-61, Highway Research Board, Washington, D.C., U.S.A., (1964).

[23] V. Ramachandran, R. Paroli and J. Beaudoin, "*Handbook of Thermal Analysis of Construction Materials"*,Noyes Publications-Williams Andrew, New York, (2003).

[24] V. Dodson, *"A study of the reaction between oxygen and mixtures of kaolinite and certain metal chlorides at elevated temperatures"*, The Ohio J. of Scie., 57(1), (1957).

[25] T. Kozík and I. Štubňa, *"Mechanical strength of the ceramic material in the dehydroxylation temperature region"*, Silikáty, 25, N3, 237-241, (1981).

[26] T. Kozík, "The temperature dependence of the electric conductivity of unfired porcelain mixture. Ceramics-Silikáty, 36, N2, 69-72, (1992).

[27] I. Štubňa and A. Trnik, *"Young's modulus of porcelain mixture after firing in the dehydroxylation region"*, Ceramics − Silikáty, 51 (2), 102-105, (2007).

[28] I. Lecomte, M. Lie´geois, A. Rulmont, R. Cloots and F. Maseri, *"Synthesis and characterization of new inorganic polymeric composites based on kaolin or white clay and on ground-granulated blast furnace slag"*, J. Mater. Res., 18 (11), (2003).

[29] Knovel International Critical Tables, Physics, Chemistry and Technology. (1st electronic ed.), (2003),

[30] B. Sonuparlak, M. Sarikaya and I. Aksay, *"Spinel Phase Formation during the 98OºC Exothermic Reaction in the Kaolinite-to-Mullite Reaction Series"*, J. Am. Ceram. Soc., 70 (11), 837-42, (1987).

[31] C. Ward and D. French, *"Analysis and Significance of Mineral Matter in Coal"*, 21st Annual Meeting of The Society for Organic Petrology, at The University of New South Wales, Sydney, New South Wales, Australia, (2004).

[32] R. Pampuch, *"Infrared study of thermal transformation of kaolinite and the structure of metakaolin"*, Prace mineral., 6, 53-70, (1966).

[33] I. Kiselev, *"Firing of kaolin and investigation of fired products"*, PhD thesis stored in ONIITECHIM, Čerkassy, No.1762178, (1978).

[34] B. Živanovič and O. Janovič, "Dehydroxylation of kaolinite", Hem. Ind., 32 (8), 512-516, (1978).

[35] L. Poppe, M. Gabor, J. Wajand and Z. Szabó, "Two-step dehydroxylation of the kaolinite", in: Proc. 1st Symp. Thermal Anal., Salford, 332–335, (1976).

[36]S.Chandrasekhar, *"Influence of metakaolinization temperature on the formation of zeolite 4A from kaolin"*, Clay Miner., 31, 2, 253-261, (1996).

[37] J. Lemaitre, A. Lronard, and B. Delmon, *"Le mecanisme de transformation thermique de la metakaolinite"*, Bull. Miner, 105, 501-507,(1982).

Table (1): Mix composition of refractory castable batches based on kaolin aggregate (K).

Sample Symbol	Kaolin Agg. Wt. %	Binding matrices		
		CAC wt. %	Spinel wt. %	
K0	90	10	0	
K1	90	8	2	Preformed spinel
K2	90	6	4	
K3	90	4	6	
K4	90	8	2	Preformed mullite
K5	90	6	4	
K6	90	4	6	
K7	90	8	2	In situ spinel (MgO + Al₂O₃)
K8	90	6	4	
K9	90	4	6	
K10	90	8	2	In situ mullite (3Al₂O₃ + 2SiO2)
K11	90	6	4	
K12	90	4	6	

Table (2): The percentage weight loss of castable sample K0

Temperature Stage (ºC)		Castable Sample K0 (Sample wt.: 23.91 mg)
Start	End	Wt. loss%
28	200	0.868
200	278	1.271
278	648	1.108
648	716	0.150
Total:		3.397 %

Table (3): The percentage weight loss of castable samples K2 and K8

Temp. Stage (ºC)		Castable Sample K2 (Sample wt.:2.289 mg)	Temp. Stage (ºC)		Castable Sample K8 (Sample wt.:4.903 mg)
Start	End	Wt. loss%	Start	End	Wt. loss%
55	188	0.094	23	203	0.601
190	291	1.202	204	283	1.062
293	437	0.119	284	603	1.039
439	594	0.052	603	667	0.604
596	665	0.254			
Total:		1.721 %	Total:		3.306 %

Table (4): The percentage weight loss of castable samples K5 and K11

Temp. Stage (ºC)		Castable Sample K5 (Sample wt.:5.208 mg)	Temp. Stage (ºC)		Castable Sample K11 (Sample wt.:1.672 mg)
Start	End	Wt. loss%	Start	End	Wt. loss%
26	193	0.397	35	208	---
195	275	1.115	211	270	0.720
276	608	0.534	273	443	---
610	673	0.523	445	649	0.028
Total:		2.569 %	Total:		0.748 %